

A Dissipative Hydrological Model for the Hotan Oasis (DHMHO)

Changsen Zhao · Bing Shen · Lingmei Huang ·
Zhidong Lei · Heping Hu · Shixiu Yang

Received: 9 May 2007 / Accepted: 11 July 2008 /
Published online: 15 August 2008
© Springer Science + Business Media B.V. 2008

Abstract Various hydrological models have been designed to simulate moisture transformation in the water-cycle system between atmospheric water, surface water, soil water and groundwater. But few have been designed specially for oases in arid desert areas where the ecology and the environment are vulnerable because of unwise water-land resources utilization. In order to analyze the moisture transformation in the Hotan Oasis in the Taklimakan Desert in China, and hence to provide scientific references for the rational exploitation and allocation of the limited water-land resources, for the purpose of ensuring that the vulnerable ecology and environment there can be gradually improved and the social economy there can develop sustainably, a dissipative hydrological model for the Hotan Oasis (DHMHO) was developed. It was an outcome of years of systematic study on the moisture transformation in arid areas and on the water-land conditions in the Hotan Oasis. Based on statistics, DHMHO introduces two empirical equations whereby we dynamically calibrated model parameters with monthly data from year 1971 to 1995. Then the calibrated parameters were used to model the moisture movement from 1996 to 2003 and thereafter rationality check and error analysis were conducted. The error analysis results show that the absolute relative errors between simulated and observed groundwater depth values are almost (11 of 12 points) within 20%, and

C. Zhao (✉)

Department of Water Resources and Environment, Sun Yat-sen University,
Guangzhou, 510275, People's Republic of China
e-mail: hzjohnson2003@163.com

C. Zhao · B. Shen (✉) · L. Huang

Xi'an University of Technology, Xi'an, Shaanxi Province,
710048, People's Republic of China
e-mail: shenbing@xaut.edu.cn

Z. Lei · H. Hu · S. Yang

Department of Hydraulic Engineering, Tsinghua University,
Beijing, 100084, People's Republic of China

those in annual watershed outflow simulation are mostly (six of eight points) within 20% with an average annual Nash–Sutcliffe Efficiency Coefficient (NSEC) of 0.80. With DHMHO and IPCC assessment, we also simulated the moisture transformation and dissipation in the Hotan Oasis from the year 2011 to 2020. Results show details of the water resources in the Hotan Oasis in the next decade and hence are expected to provide scientific references for establishing rational exploitation and allocation policies on the local water–land resources in the future.

Keywords DHMHO · Moisture transformation and dissipation · Water balance · Hotan Oasis

1 Introduction

In developing arid desert regions, demand for fresh water resources usually rises sharply with the development of economy due to lack of advanced technologies. Conflicts between water users of up and down reaches, of left and right banks and of ecology, economy and society, are becoming more and more severe. The Hotan Oasis in China is the case. Because of unreasonable long-term water–land resources exploitation, quantity of available fresh water resources in the oasis becomes less and less, quality of ecology and environment there is degenerating. According to Wang et al. (2003), the ecology and environment in the Hotan Oasis falls into the category of the medium fragility. In such a situation, it is most urgent to make clear the local water resources status quo and further the moisture movement rules in the local water-cycle system. Only based on that can the residents in the oasis act properly in making policies on future exploitation and allocation of local water–land resources, and hereby improve the ecology and environment quality. As such, their living standard may be elevated and therefore the Oasis is expected to have a sustainable development.

Hydrological models can be used to simulate atmospheric water, surface water, soil water and groundwater in a water-cycle system. It seems so far to be the most efficient mathematical approach to give people an understanding of the details about water resources in oases in arid desert regions. Thus, the focus seems to be to choose or design a proper hydrological model to undertake the above tasks.

Hydrological models, the principle of which is the water-balance theory, started with the Sherman Unit Hydrograph in the 1930s, boomed in the period from the 1960s to the 1980s when hundreds of models sprung up. With advances in computer technologies and in interdisciplinary fields after the 1980s, research on semi-distributed or distributed hydrological models has become a hot issue. However, most hydrological models were designed for humid or semi-humid areas and few of them can be adopted to correctly simulate the moisture movement and transformation in such arid desert areas as the Hotan Oasis. For example, in China, there are the lumped Shanbei model (Zhao 1984) for the semi-arid Loess Plateau, the distributed DTVGM (Xia 2002; Xia et al. 2005) for semi-humid areas etc. during this period; globally, there are many models available to represent rainfall–runoff relationships:

STORM (US Army Corps of Engineers 1997), an urban watershed model, is capable of calculating loads and concentrations of water quality variables; KINEROS (Hernandez et al. 2000), a physically based distributed model for semi-arid regions,

describes the processes of surface runoff from small watersheds; IHACRES (Jakeman et al. 1990; Dye and Croke 2003), a simple lumped conceptual model for semi-arid regions, requiring minimal input data, has been applied widely all over the world (Chai et al. 2006); SMADA (Wanielista et al. 1997), designed to generate watershed hydrographs and route hydrographs through ponds using inventory routing, has been used to estimate the runoff generated from different storms; Technical Release 20: Computer Program for Project Formulation Hydrology (TR-20; SCS 1983), a hydrologic model for the simulation of direct runoff hydrographs resulting from natural or synthetic rainfall dropping into a watershed, can be used to model complex watersheds with multiple sub-areas, channel reaches, and reservoirs (Casey 1999); Wang et al. (2006) proposed a storm response overland flow model with laboratory experiments, Li and Gowing (2005) presented a daily water balance model to simulate the performance of irrigation systems, but they do not account for groundwater and soil water some details of which are often required in the exploitation of underground water resources in arid desert areas;

MODFLOW is a computer program that numerically solves the three-dimensional ground-water flow equation for a porous medium by using a finite-difference method (Harbaugh et al. 2000) however, it mentions little about surface water, let alone water transformation in a water-cycle process.

To avoid the shortcomings discussed above, some scholars combined KINEROS and SWAT (Borah and Bera 2003) to characterize the runoff response of the semi-arid watershed due to changes of land cover (Hernandez et al. 2000). But in a desert area like the Hotan Oasis, all of the methods mentioned above doom to fail because all of them have such an assumption as that rainfall may produce surface or soil runoff. This assumption, however, is unable to be satisfied in the Hotan Oasis where, a brand-new water transformation and dissipation law different from that in (semi-) humid or semi-arid areas might exist.

Refsgaard et al. (1998) integrated MIKE SHE, MIKE 11, MIKE 21 and DAISY to study the environmental assessment in connection with the Gabcikovo hydropower scheme; Chen et al. (2005) proposed a water budget model to estimate the infiltration, runoff, evapotranspiration and recharge in vadose zone; Loukas et al. (2007) combined a hydrological model, a reservoir operation model with methods for the estimation of water demands to evaluate the sustainability of water resources management strategies in two basins in Greece, but their essential is still the traditional rainfall–runoff relationship, and cannot be applied in the Hotan Oasis where runoff is not produced from the rainfall in the local plain area but from the rainfall and glacier melted water in the upstream mountain outside the Hotan Oasis.

The lack of a long-term gauged stations network in arid desert areas seems to have limited our knowledge of the rules of moisture movement and transformation. Therefore, no hydrological model has been designed to accurately simulate the water movement in the local water-cycle system of arid desert areas. That consequently hinders the local people's ability to use and allocate water–land resources in an intelligent way and consequently a series of ecology and environment problems occur (taking the Hotan Oasis as an example, Wang et al. 2003). So, the accumulation of data on water movement and moisture transformation, on climate, on geology etc. in arid desert areas may be the sole way to gain access to the hydrological model, which is needed to provide scientific bases on which local development policies can be established wisely.

After years of systematic study on the rule of the moisture transformation in arid desert areas and on the water–land conditions in the Hotan Oasis, based upon the analysis of the accumulated data, we developed the Dissipative Hydrological Model for the Hotan Oasis (DHMHO) from an arid plain oasis model created by Tsinghua University, Xi'an University of Technology and Xinjiang Agricultural University (Hu et al. 2004; Tang 2003; Tang et al. 2004; Zhao 2005). With DHMHO, we simulated the water cycle process in the Hotan Oasis. The simulations can bring people a clear knowledge of the water resources status quo, which will be greatly significant in guiding Hotan Oasis residents to establish reasonable exploitation and allocation policies on water-land resources, thereby in improving the quality of the local ecology and environment and the local living standard.

If there exist similar underlying conditions as those in the Hotan Oasis, e.g. in Arab arid desert areas, DHMHO can be used to simulate the moisture movement in the local water-cycle system. With the simulation details, policy-makers can act more reasonably in establishing water–land resources exploitation and allocation policies, which will certainly benefit the development of the local social economy.

2 Description of Research Areas

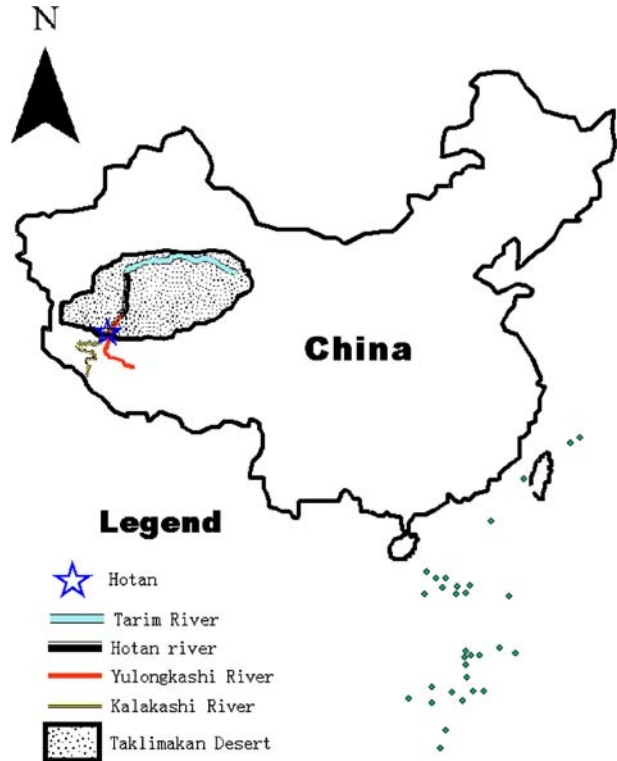
Hotan, in the northwest of China, was a crucial transport hub in the ancient 'Skill Road' which acted as a bridge of culture and economy between ancient China and ancient European.

The Hotan Oasis lies south of the Taklimakan Desert—in the northwest of China. The greatest river crossing the oasis is the Hotan River, as shown in Fig. 1. The Hotan River has two branches—the Kalakashi River and the Yulongkashi River. They converge into the Hotan River in Kuoshilashi. The Hotan River winds its way through the Taklimakan Desert for 319.0 km before flowing into the Tarim River. A control hydrometric station—Xiaota lies in the place 16 km before the converging site. In the upper reach of the two branches, there are two hydrometric stations—Wuluwati (171 km upstream from Kuoshilashi) on the Kalakashi River, and Tonguziluo (204 km upstream from Kuoshilashi) on the Yulongkashi River; two water-diverting canal heads are located on the two branches (Fig. 2).

The local climate falls into the category of continental warm temperate monsoon climate, with total rainfall quantity being 7.7–91.0 mm per year, and with total evapotranspiration quantity being 1,938–2,791 mm per year.¹ The intense evapotranspiration brings about severe drought in the oasis—the aridity index in the Hotan Oasis ranges from 25 to 842.¹ The study of Shen et al. (2003) on the Hotan Oasis water-cycling characteristics shows: (1) There is a rising tendency in annual temperature, and the local climate is in the course of warming up; (2) intense as the evapotranspiration maybe, there exists no obvious rising tendency in annual humidity, the reason for which may be that the oasis is divided and surrounded by arid deserts so that water vapor mostly dissipates into the desert and contributes little

¹Data source: Department of Hydraulic Engineering of Tsinghua University etc. Report of China Xinjiang Tarim Basin no. 2 Project-Study of water–salt balance and its simulation model in Tarim Basin, 2004,10.

Fig. 1 Sketch of Hotan location



to a rise in oasis humidity; (3) the insignificant rainfall in the Hotan Oasis is unable to produce surface runoff which, in the river, is mainly recharged by rain water and snowmelt water from the upper mountain region—yet, the runoff quantity at the outlets of the upper mountain regions has been decreasing; (4) the annually slight rainfall can only moisten the soil surface, which reduces the salinity of surface layer and hence the salt in the deeper layer moves upward along with up soil moisture to make the salinity of surface layer higher, therefore, the soil salinization in the oasis becomes severer and severer.

In the Hotan Oasis, irrigated farming is the principal human activities. Its development depends mainly on the surface water supply. Groundwater sources were historically little used due to a lack of electricity and other resources required by groundwater-pumping. Because of the absence of watershed management on water-land resources, people living upstream divert river water excessively for irrigation, resulting in an increase of cropland area and a rise of the groundwater table as well. The latter is the chief cause of soil salinization. Those living downstream suffer from draught because of insufficient river water. As a result, a wide area of cropland downstream is being abandoned and gradually desertifying due to lack of irrigation water. On the whole, the long-term unreasonable utilization of water-land resources hinders agricultural development and causes the local ecology and environment to degenerate. Wang et al. (2003) indicate that the ecology and the environment in the Hotan Oasis fall into the category of medium fragility and is an ecological and environmental malfunctioning area.

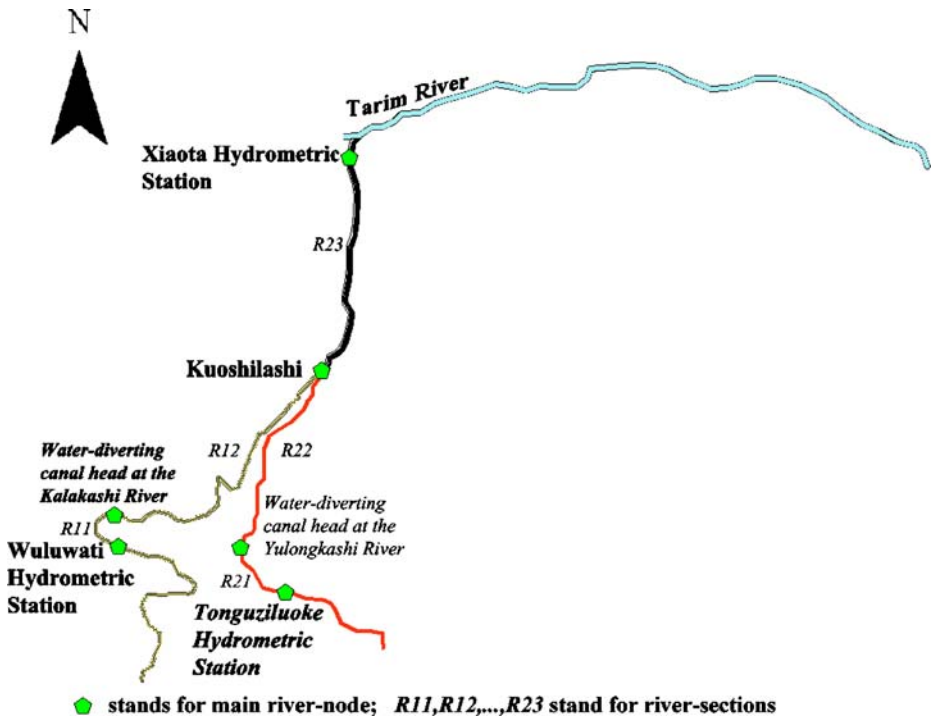


Fig. 2 Sketch of main river-nodes and river-sections in the Hotan River

3 Historically Hydrological Data in the Hotan Oasis

3.1 Air Temperature

From year 1954 to 2003, the mean annual air temperature fluctuated around the value of 11.96°C. The minimal value was 11.06°C and the maximal one was 12.90°C.

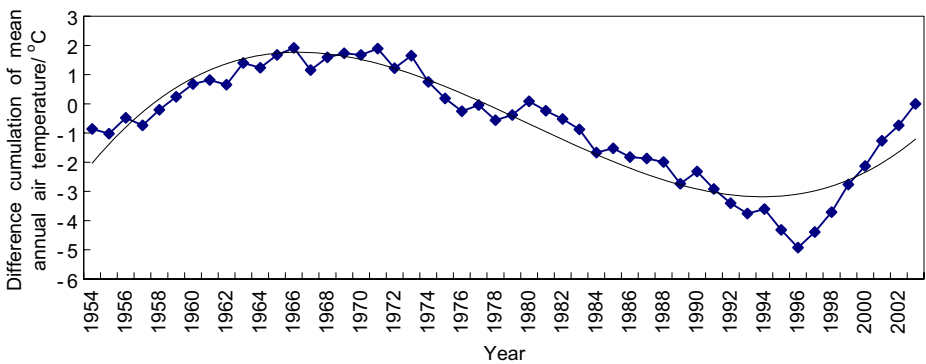


Fig. 3 Difference cumulation curve of mean annual air temperature in Hotan Oasis. Difference here means that of a sequence element value from the average value of the sequence

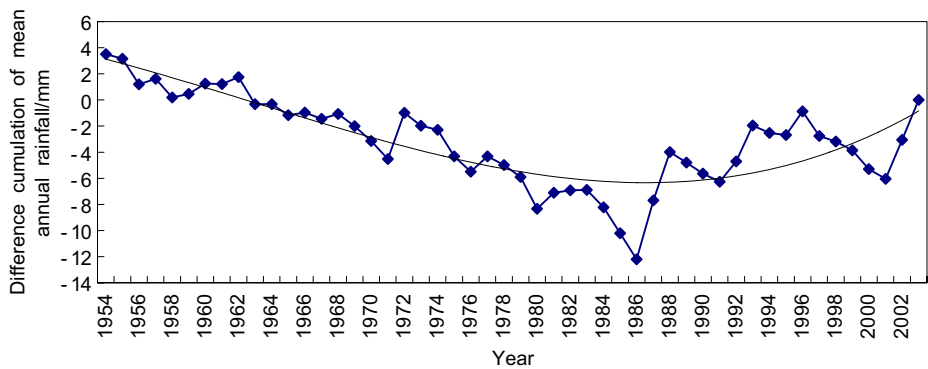


Fig. 4 Difference cumulation curve of mean annual rainfall in Hotan Oasis

From Fig. 3, one can find the trend of mean annual temperature: From year 1954 to 1966 was the rising period; from year 1966 to 1996 was the declining period with a little tiny fluctuation; after the year 1996, mean annual air temperature rose again. According to Shen et al. (2003), air temperature in the Hotan Oasis had a notable rising tendency especially in winter; the mean annual air temperature there, was predicted to be 13.3°C in the year 2050, which will to some degree affect the daily life and production of local residents.

3.2 Precipitation

The mean annual rainfall in the Hotan Oasis fluctuated around 3.09 mm; the minimum value was 0.64 mm and the maximum one was 7.58 mm, which means that averagely there was 3.09 mm atmospheric water falling onto ground surface every month. Figure 4 tells us that from year 1954 to 1986, the precipitation had a declining trend while from year 1987 to 2003, it had a slight rising trend.

3.3 Evapotranspiration

The mean annual evapotranspiration fluctuated around 198.78 mm which means that averagely there was 198.78 mm water going up into the Hotan Oasis' air every month; the minimum value was 161.54 mm and the maximum one was 232.60 mm. Figure 5 suggests that from year 1955 to 1963, the evapotranspiration had a rising trend while from year 1984 to 2003, it had a declining trend and from year 1964 to 1983, it had a slight rising tendency.

3.4 Humidity

The mean annual relative humidity in the Hotan Oasis fluctuated around 47.08%; the minimum value was 37.00% and the maximum one was 60.42%. From year 1954 to 1970, the relative humidity in the Hotan Oasis had a declining trend while from year 1971 to 2003, it had a slow rising trend (Fig. 6).

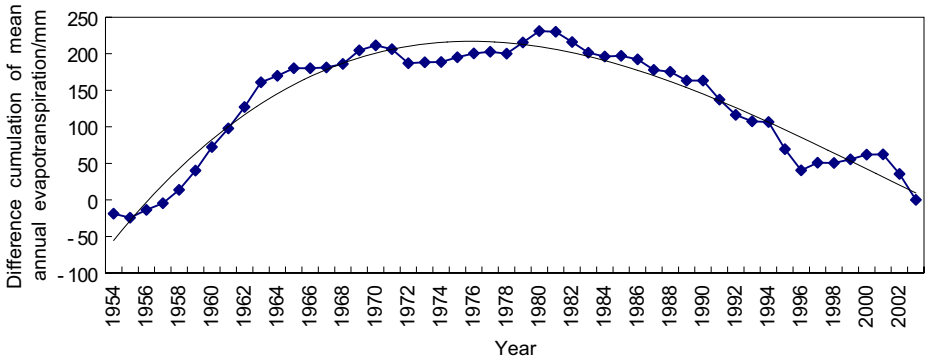


Fig. 5 Difference cumulation curve of mean annual evapotranspiration in Hotan Oasis

Comparing Figs. 3, 4, 5, 6 with each other, one can draw the following conclusions:

1. In the period from year 1954 to the middle of 1960s, mean annual air temperature and mean annual evapotranspiration had rising tendencies while mean annual rainfall and mean annual relative humidity had declining ones;
2. In the period from the middle of 1960s to the middle of 1990s, the tendencies of the above four indices were: temperature and rainfall declined while the other two rose;
3. In the period from the middle of 1990s to year 2003, their tendencies were not very clear: temperature and relative humidity rose, rainfall firstly declined and then rose while evapotranspiration firstly rose and then declined.

Further analyses suggest: mean annual rainfall had always opposite tendency to that of mean annual evapotranspiration; in the period before the middle of 1990s, the tendencies of mean annual temperature and mean annual relative humidity were opposite while in the period after the middle of 1990s, the two indices had roughly the same tendency.

Above analyses indicate that there may exist different water cycle mechanism in an arid desert area from in a humid area. For example, in a humid area, rainfall is large enough to produce runoff, because of increment in which, soil moisture,

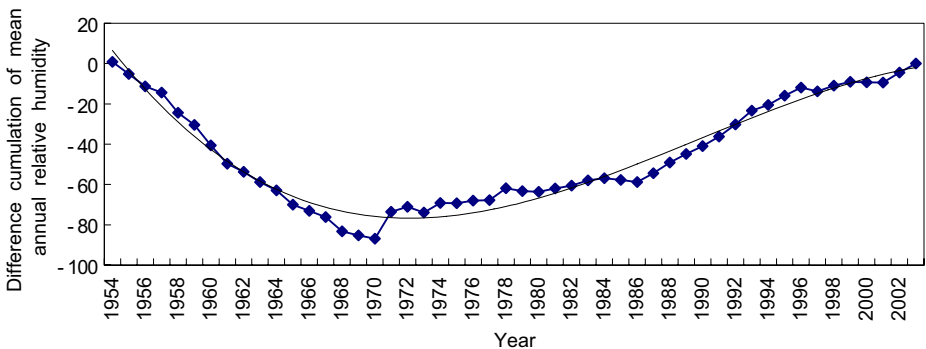


Fig. 6 Difference cumulation curve of mean annual relative humidity in Hotan Oasis

groundwater table and water surface area increase. This ultimately makes evapotranspiration quantity go up. Differently, in an arid desert area, rainfall is too few to act the same as in a humid area. It can only moisten the air and soil surface in an arid desert area. Its work on the air moisture may be the reason of anti-correlation existed between rainfall and evapotranspiration in the Hotan Oasis, as illustrated in Figs. 4, 5, 6. Above discussed implies that there may exist great differences in the basis of hydrology in an arid desert area from in a humid area.

3.5 Runoff

The Hotan River runoff is the base of all human activities in the Hotan Oasis. The size of the oasis varied with the capacity of the surface runoff in the history. Glaciers are the most important recharging source of the Hotan River runoff. There are totally 3,318 glaciers in the upstream of the Hotan River. Total glacial storage capacity is 566.42 km^3 among which 72.4% belong to the Yulongkashi River and 27.6% to the Kalakashi River. Glacial meltwater accounts for a larger proportion of the runoff of Yulongkashi River than that of Kalakashi River (Table 1).

Table 1 gives sources of the two branches of the Hotan River, which indicates: averagely the annual runoff of the Yulongkashi River ($22.33 \times 10^8 \text{ m}^3$) is greater than that of the Kalakashi River ($21.55 \times 10^8 \text{ m}^3$); glacial meltwater account for a larger proportion in the runoff of the former (64.9%) than in that of the latter (54.1%); groundwater recharges 18.1% of the Yulongkashi River runoff while 23.8% of the Kalakashi River runoff, which maybe the reason why the annual runoff of Yulongkashi River varies more drastically ($C_v = 0.22$) than that of Kalakashi River ($C_v = 0.18$); rainfall in the mountain areas of Yulongkashi River accounts for a smaller proportion (17.0%) than that of Kalakashi River (22.1%).

Figure 7 is the annual runoff process of the Hotan River. Wuluwati Hydrometric Station measures the inflow of Kalakashi River, and Tonguziluoke Hydrometric Station measures that of Yulongkashi River. The annual runoff process of Kalakashi River (Wuluwati) is similar with that of Yulongkashi River (Tonguziluoke): the mean value of the annual inflow of Kalakashi River is $21.55 \times 10^8 \text{ m}^3$ while that of Yulongkashi River is $22.33 \times 10^8 \text{ m}^3$; the minimum values are both appeared in the year 1965 and the maximum in the year 1961. Therefore, the total annual inflow process of Hotan River is similar with that in its two branches with the minimum values and the maximum values appeared in the year 1965 and 1961 respectively. However, because of intense human activities in the Hotan Oasis, the annual outflow process in the downstream of the Hotan River (Xiaota) differs greatly from that of inflow with an average value of $10.55 \times 10^8 \text{ m}^3$, the minimum value appearing in the year 1993 and the maximum value in the year 1978. Also, Fig. 7 indicates that the inflow and the outflow of the Hotan River both have a declining trend on the whole.

Table 1 Sources of Hotan River runoff

Branch name	Total runoff (10^8 m^3)	From glacier (%)	From groundwater (%)	From precipitation (%)	C_v
Yulongkashi River	22.33	64.9	18.1	17.0	0.22
Kalakashi River	21.55	54.1	23.8	22.1	0.18

C_v Annual variation coefficient of the total runoff, which suggests the total runoff of the Kalakashi River is stabler than that of the Yulongkashi River

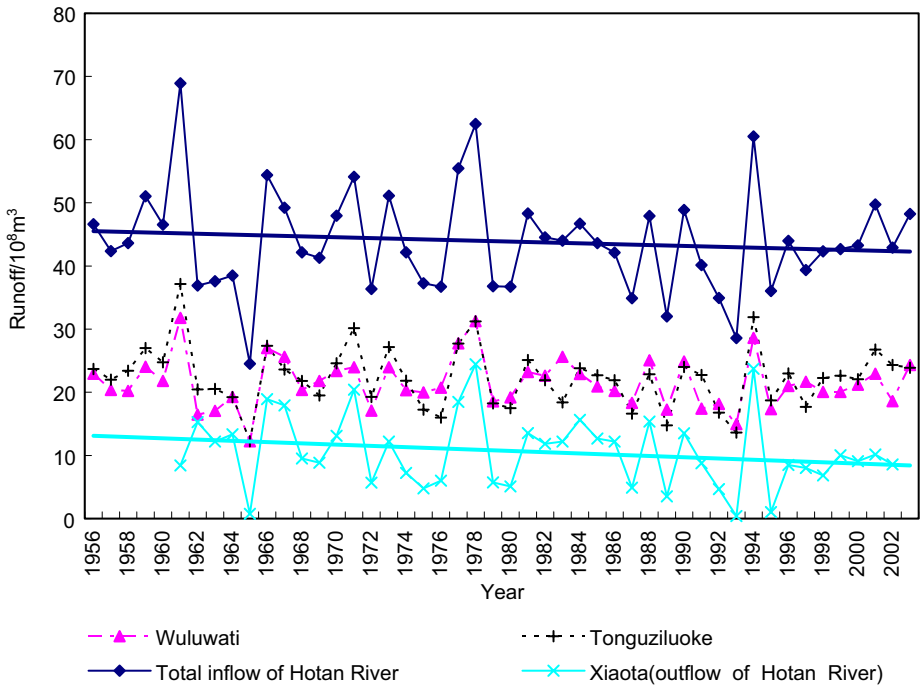


Fig. 7 Runoff of Hotan River. Wuluwati and Tongguziluo are two control hydrometric stations upstream; Xiaota is the sole control hydrometric station downstream; two straight lines show trend of their series

3.6 Water Diversion Quantity

Water diversion quantity from the Hotan River changed little while the total inflow of the Hotan River had a total trend of slightly declining (Fig. 8).

4 Description of DHMHO

4.1 Some Model-Related Concepts

The hydrological concepts in arid desert areas should differ from those in humid or semi-humid areas because of diversities in climate, geology, topography, human activities etc. For example, here we consider the definition of the so-called watershed in arid desert areas as an area within which a water body, such as a river, a lake etc., supplies surface water to users or collects surface water from their sources. Moreover, the ‘watershed’ in arid desert areas has no fixed boundaries (Tang 2003).

The dissipation in DHMHO refers to the reducing process of surface water quantity. In the Hotan Oasis, it means that surface water, recharged by Kunlun Mountains’ rain and snowmelt water, flows from higher to lower places and is bit by bit diverted for agricultural use. This water eventually reaches the atmosphere by way of evapotranspiration, either directly from the water surface or indirectly from

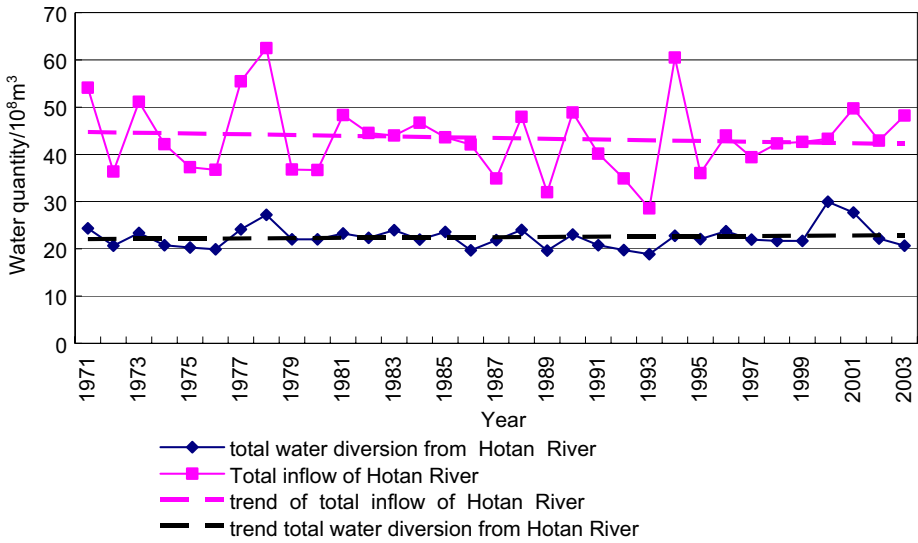


Fig. 8 Total water diversion from Hotan River and total inflow of Hotan River

soil and vegetation after surface water has seeped into underground (Tang 2003; Hu et al. 2004; Tang et al. 2004; Zhao 2005).

Usually in humid areas, the recharge process and discharge process happen at almost the same place. The recharge areas can not be distinguished from discharge areas because in a humid watershed, rainfall is often greater than evapotranspiration and is enough to produce runoff. While in arid desert areas the former can clearly be distinguished from the latter because recharge areas, the surroundings of the upstream mountains, witness slight evapotranspiration whereas discharge areas, the middle- or down-stream water-use areas such as the Hotan Oasis, get slight rainfall which is not enough to produce runoff under the specific underlying conditions in arid desert areas.

4.2 Model System

DHMHO can achieve the goal of integrating the four forms of water including atmospheric water, surface water, soil water and groundwater into a whole system. In this system, based on the input data consisting of those from geology, hydrology and meteorology etc., model variables are calculated dynamically and at last the details pertaining to the four forms of water are outputted. The outputs of the model can help local people become familiar with the moisture transformation process and water resources status quo in their living areas and use water-land resources more prudently.

Based on the facts of the research areas, in the model we designed five modules including a river module, a reservoir module, an irrigated land module, a non-irrigated land module and a groundwater module. Surface water in different water bodies is connected via a canal system and groundwater in different spots by underground lateral seepage. This model structure is shown in Fig. 9.

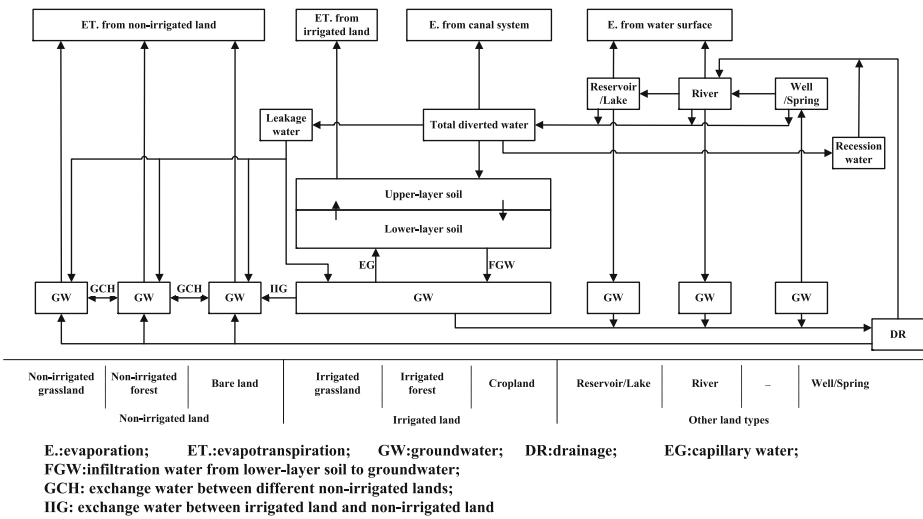


Fig. 9 Structure sketch of DHMHO

In Fig. 9, evapotranspiration from cropland, forest or grassland and evaporation from bare land or water surface are simulated respectively in the relevant modules; recession water, consisting of drainage from irrigated land and leakage-water from canal system halfway due to poor canal system management, returns finally to the Hotan River with higher salinity. After having flowed back into the river, the recession water becomes one part of the river water and is taken into account in the river water balance module.

4.2.1 River Module

In this module, the whole river is initially divided into different river-sections by main river-nodes which are chosen from among all nodes distributed over the river course according to the node data status (e.g., whether there are enough data required by the model) and the socio-economic importance (e.g., a water-diverting canal head, a branch-influx joint etc.). Taking the Hotan River as an example, we can divide it into five river-sections (R11, R12, . . . , R23) by six main river-nodes including Wuluwati Hydrometric Station, Tonguziluoke Hydrometric Station, the water-diverting canal head in the Kalakashi River, the water-diverting canal head in the Yulongkashi River, the Kuoshilashi node and the Xiaota Hydrometric Station, as shown in Fig. 2.

Then we take one month as time interval and calculate outflow—RFO one river-section after another according to Eq. 1, taking the outflow of the upstream river-section (s) as the inflow of the contiguous downstream one.

$$PP + RFI - RFO - RDI - REV - RG + RGG - RSS + \varepsilon = 0 \quad (1)$$

where:

PP rainfall quantity calculated from the observed value at weather stations ($10^4 \text{ m}^3/\text{month}$). It is often little in the Hotan Oasis, hardly producing runoff,

and is usually omitted compared with huge evapotranspiration quantity there;

- RFI* inflow of the river-section, measured input data ($10^4 \text{ m}^3/\text{month}$);
- RFO* outflow of the river-section, output of DHMHO ($10^4 \text{ m}^3/\text{month}$);
- RDI* runoff diverted from the river-section for the purpose of irrigation, measured input data ($10^4 \text{ m}^3/\text{month}$);
- REV* evaporation from water surface in the river-section, calculated in DHMHO ($10^4 \text{ m}^3/\text{month}$). $REV = RWIDTH \times RLEN \times E_0$, among, *RWIDTH* is the mean width of the calculating river-section, m, $RWIDTH = K_r \times (a * RF + b)$, K_r , a and b are coefficients; *RLEN* is the length of the calculating river-section and can be obtained from a map or satellite image, m; E_0 is evaporation from water surface, $E_0 = k' \times E'_0$, E'_0 refers to the measured evaporation, meters per month, k' is the transformation coefficient from measured to actual value;
- RG* seepage in the river-section, calculated in DHMHO ($10^4 \text{ m}^3/\text{month}$). $RG = \sigma + \tau \times RF + \nu \times RF^2$, among, σ , τ , ν are the empirical coefficients calibrated with the measured seepage data and inflow data; *RF* is the inflow of the calculating river-section, measured data or the calculated outflow of the upstream river-section, m^3/s ;
- RGG* recession water consisting of leakage water from canal system and drainage water from irrigated land, calculated in DHMHO ($10^4 \text{ m}^3/\text{month}$);
- RSS* change in water storage in the river-section within the time interval, calculated in DHMHO ($10^4 \text{ m}^3/\text{month}$). $RSS = a \frac{RWIDTH_t + RWIDTH_{t-1}}{2} \times RLEN \times \ln(RF_t / RF_{t-1})$, among, t stands for the current calculating interval, $t - 1$ is the previous calculating interval, month; a is a coefficient calibrated with measured data;
- ε calculation error ($10^4 \text{ m}^3/\text{month}$).

In the water balance process, we adopt the iterative algorithm to adjust the variables in Eq. 1 so as to avoid such unreasonable results as evaporation, seepage, and outflow in the river-section being less than 0. First, we introduce a variable *rsstotal* to accumulate the total water storage in the river-section continuously from the very beginning of calculation time and ensure that *rsstotal* is greater than or at least equal to 0 if the dissipative variables—evaporation, seepage and outflow are greater than 0. If there is no water left in the river-section, there will exist practically no evaporation, seepage and outflow. The water storage there will in fact never be minus and if it becomes minus, a water-deficit in the river-section (*wd* in Fig. 10) occurs, which means that the dissipative variables need to be adjusted. If a water deficit occurs, we proportionally reduce the dissipative variables to make up for it. If there is a variable in the dissipative ones less than 0 after being adjusted, we readjust the relevant variables and iterate the water-balance process till the dissipative variables in Eq. 1 and total water storage in the river-section are greater than or equal to 0, as shown in Fig. 10.

4.2.2 Reservoir Module

Reservoirs in the Hotan Oasis lie in the plain areas where loam and sandy loam are dominant soil types, in addition, most reservoirs were built in 1950s or 1960s.

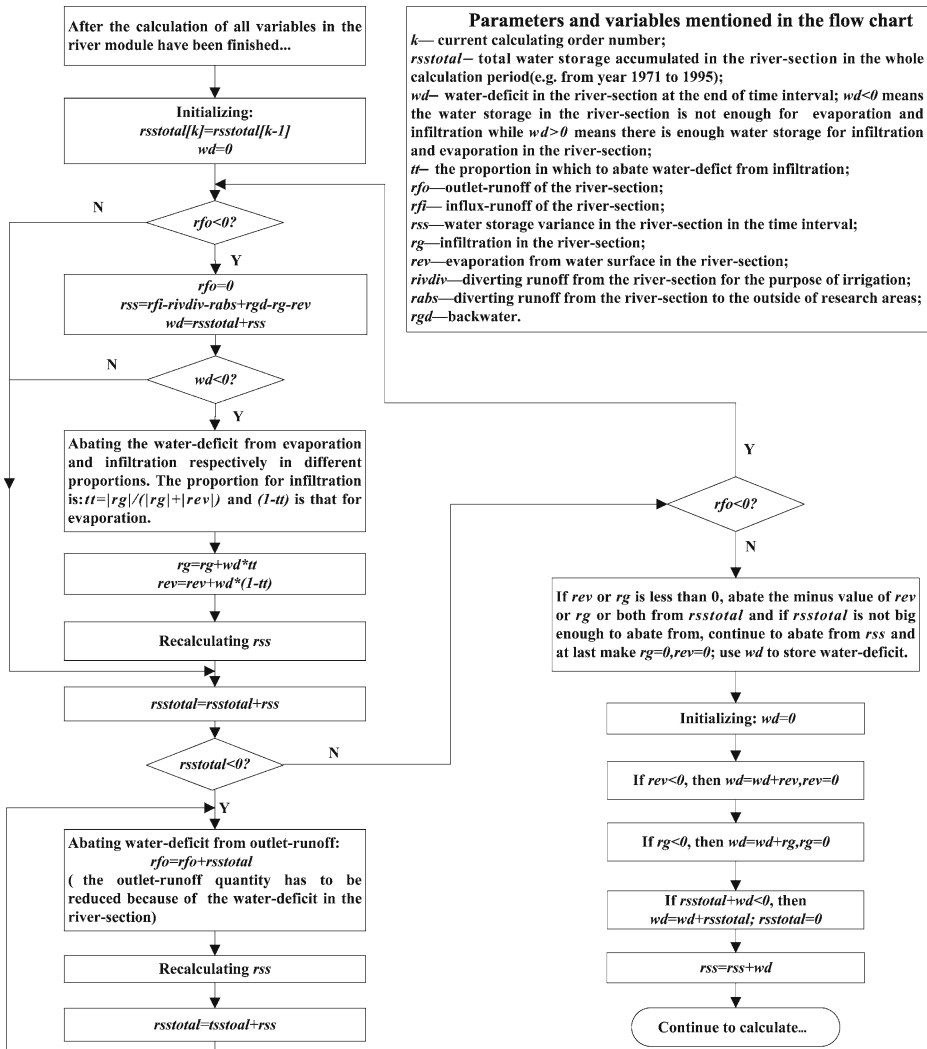


Fig. 10 Iteration adjustment flow chart in river water-balance process

Therefore seepage and evaporation of reservoirs are the main dissipative variables which historically account for 30~70% of the inflow of reservoirs. With the improvement of water-saving awareness, people in the Hotan Oasis will surely do their best to reduce the percentage in future.

A reservoir or lake is a relatively independent water balance system. The main dissipative items are water quantity diverted from a reservoir to irrigated areas, reservoir evaporation and seepage. In this module, we first calculate the evaporation and seepage and then calculate the outflow of the reservoirs with Eq. 2.

$$PP + SRI - REV - SSP - SRS - SRO = 0 \tag{2}$$

where:

- SRI* inflow of reservoir ($10^4 \text{ m}^3/\text{month}$);
SRO outflow of reservoir ($10^4 \text{ m}^3/\text{month}$);
REV evaporation from reservoir ($10^4 \text{ m}^3/\text{month}$). $REV = f_{rev} \times RVOL \times E_0$, among, $RVOL$ is the mean storage capacity of the calculating reservoir, $RVOL = (RVOL_0 + RVOL_1)/2$, $RVOL_0$ is the storage capacity in the begin of the calculating interval and $RVOL_1$ is that in the end of the calculating interval, $RVOL_1 = \frac{(2 - f_{rev} \times E_0 - f_{seep}) \times RVOL_0 + 2(SRI - SRO)}{2 + f_{rev} \times E_0 + f_{seep}}$, m^3 ; f_{rev} stands for the slope of the reservoir storage-area curve, and because the old reservoirs in the Hotan Oasis usually lack storage-area curve, we simplify it as a straight line;
SSP seepage of the reservoir ($10^4 \text{ m}^3/\text{month}$). $SSP = f_{seep} \times RVOL$, f_{seep} is a coefficient for seepage;
SRS change in water storage of the reservoir ($10^4 \text{ m}^3/\text{month}$). $SRS = RVOL_1 - RVOL_0$;

4.2.3 Irrigated Land Module

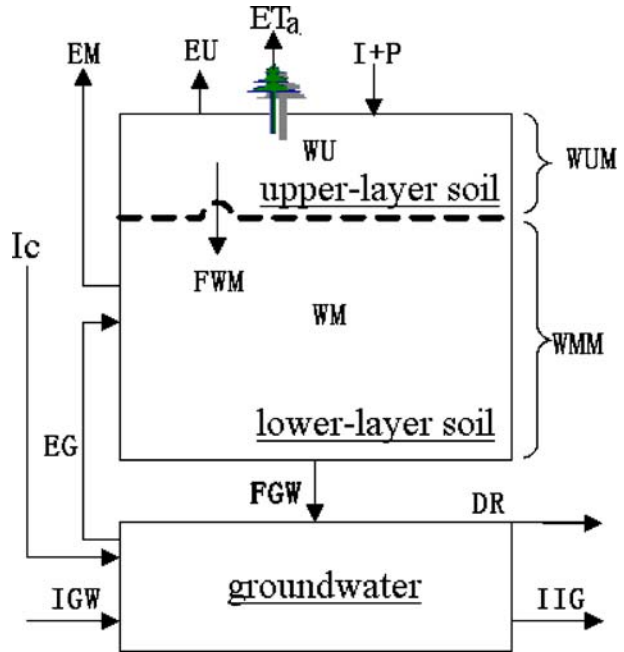
The irrigated land here consists of all cropland and the forest land or grassland which needs irrigating. In this module, the whole soil layer in irrigated land is divided into three layers vertically including upper-layer soil, lower-layer soil and groundwater layer (as shown in Fig. 9). All water, except for the quantity directly evaporating from the water surface in areas between individual plants, seeps into upper-layer soil and then turns into soil moisture after having been diverted into irrigated land. Some soil moisture is absorbed by plant roots and transported to stems and leaves for plant's growth and transpiration; the rest percolates into the lower-layer soil after the upper-layer soil is saturated, and the remainder into the groundwater after the lower-layer soil is saturated. There exist continuous vertical moisture exchanges between the three layers under the control of the soil water potential including the gravity potential, the pressure potential, the matric potential, the solute potential and the temperature potential (Lei et al. 1988)—the upward moisture is the capillary water and the downward one is the percolation water, as shown in Fig. 11. Also, there exist continuous horizontal moisture exchanges between different adjacent irrigated lands under the control of the soil water potential. The upper-layer soil and the lower-layer soil have the capacity to store water and adjust its level. Especially the upper-layer soil, where often plant roots are active, has a strong adjustment mechanism and a considerable water storage capacity, and is therefore usually referred to as the 'soil reservoir' by scholars (e.g. Meng and Xia 2004).

In this module, the model encompasses main recharging items including irrigating water, rainfall, groundwater lateral seepage and canal leakage, and main dissipative items such as evapotranspiration from irrigated vegetation, evaporation from upper-layer soil, evaporation from lower-layer soil, groundwater drainage and groundwater exchange between irrigated land and non-irrigated land, as shown in Fig. 11.

In this module,

- I* irrigating water, mm/month . $I = R \times \eta$, R is the total diverted water, measured at water-diverting canal head, millimeters per day; η is the water use efficiency of canal system;
P rainfall, mm/month ;

Fig. 11 Moisture movement in irrigated land (Tang 2003). In irrigated land, total evapotranspiration has three parts: evapotranspiration from vegetation, evaporation from upper-layer soil and that from lower-layer soil. Usually, energy is firstly used to transpire and evaporate the moisture in the vegetation and the upper-layer soil, and if there is any energy left to be used to evaporate the moisture in the lower-layer soil



- ET_a the evapotranspiration from irrigated vegetation, millimeters per month. $ET_a = ET_0 \times Kc \times Sc$, ET_0 is the potential evapotranspiration capacity, calculated with the FAO Penman–Monteith method (1994; Otlés and Gutowski 2005), millimeters per day; Kc is the crop coefficient which varies with kind and growing stage of plant; Sc is the water-supply coefficient, $Sc = (\text{actual water-supply quantity})/(\text{water-demand quantity})$;
- EU the evaporation from upper-layer soil, millimeters per month. $EU = K \times ET_0$, K is the evaporation coefficient of upper-layer soil, varying with vegetation type. If the land is covered by vegetation, EU is often omitted because evapotranspiration from vegetation constitutes most part of the total evapotranspiration and at this time we merely take into account the evapotranspiration from vegetation;
- EM the evaporation from lower-layer soil, millimeters per month. $EM = Ks \times ET'$, Ks is evaporation coefficient, $Ks = WM/WMM$, where WM refers to the actual moisture storage in lower-layer soil and WMM the maximum soil moisture content, WM is usually given an initial value and is iterated in the model; ET' is the residual evaporation capacity which equals to the difference between total evaporation capacity and actual evaporation from upper-layer soil, mm/day;
- DR is the groundwater drainage, millimeters per month;
- EG is the upward capillary water, millimeters per month. $EG_i = \min(E_0 \times e^{\alpha_i(H_i-r_i)}, \beta_i \times (H_i-r_i)^\gamma)$, i stands for soil type; E_0 is evaporation from water surface, millimeters per day; H is the groundwater depth, output value, meters; r is the mean vegetation root depth varying with growth time, meters; α, β, γ are the evaporation coefficient varying with soil type;

- I_c is the canal system leakage, mm/month. $I_c = R \times (1 - \eta) \times (1 - tceff) \times pgc$, $tceff$ is the coefficient of leakage-water in canal system; pgc is the leakage coefficient of canal water;
- IGW is the groundwater side gain, mm/month;
- IIG is the groundwater exchange between irrigated land and non-irrigated land, millimeters per month.
- WUM the water storage capacity of upper-layer soil, while WMM that of lower layer, millimeters;
- WU is the actual water storage of upper layer, WM that of lower layer, millimeters;
- FWM is the seepage from upper-layer soil to lower-layer soil, FGW that from lower-layer soil to groundwater, millimeters per month;

If $WU + (I + P) > WUM$ then we can get: $FWM = WU + (I + P) - WUM$, $WU = WUM$, or else, we can get: $FWM = 0$, $WU = WU + (I + P)$; If $ET > WU$ then we get: $WU = 0$, $ET' = ET - EU$, or else, we get: $EU = ET$, $WU = WU - EU$, $ET' = 0$. Among, ET is the total evaporation capacity, calculated with the FAO Penman–Monteith method (1994; Otles and Gutowski 2005), millimeters per day.

If $WM + FWM > WMM$ then we can get: $FGW = WM + FWM - WMM$, $WM = WMM$, or else, we can get: $FGW = 0$, $WM = WM + FWM$; If $WM + EG > WMM$ then we get: $EG = WMM - WM$, $WM = WMM$, or else, we get: $WM = WM + EG$.

4.2.4 Non-irrigated Land Module

The non-irrigated land includes the forest land and the non-irrigated grassland, the bare land etc. Because by and large no water is diverted into non-irrigated land for the purpose of irrigation, almost all moisture in the vadose zone comes from upward capillary moisture recharged by groundwater—hence, the soil layer over groundwater layer can be regarded as the conducting layer of the groundwater and has a relatively stable soil moisture content (Tang 2003; Zhao 2005). Therefore, the change in soil moisture water storage can be omitted, and mere the change in groundwater storage is considered. Because of the reasons mentioned above, the soil layer over the groundwater layer, different with in irrigated land, is not taken into account yet, as shown in Fig. 9. The dissipative items here are the evaporation or transpiration from land surface. It may greatly affect the groundwater table in non-irrigated land.

In this module, the main recharging items include leakage water from canal system (I_c), that from river (RG) and that from reservoir (SSP); groundwater drainage from irrigated land (DR) and groundwater exchange between irrigated land and non-irrigated land (IIG). The main dissipative items encompass evaporation from bare land surface, marsh etc. (NE), as well as evapotranspiration from non-irrigated vegetation (ET_b).

Among, $SSP = fseep \times RVOL$, $fseep$ is the seepage coefficient of a reservoir, $RVOL$ is the mean volume of a reservoir. $NE_i = ET_i * e^{\alpha_i(H_i - r_i)}$, i stands for the land type such as barren land, marsh etc., from investigation or satellite image; ET_i is the potential evapotranspiration capacity of the i th type of surface, calculated with the FAO Penman–Monteith method (1994; Otles and Gutowski 2005), millimeters per day; α_i is the evaporation coefficient of the i th type of surface; H_i is the groundwater

depth in the i th type of land, output value, meters; r_i is the mean root depth in the i th type of land, varying with the vegetation kinds, meters. $ET_b = ET_0 \times K'$, K' is the evapotranspiration coefficient varying with kind and growing stage of vegetation, calibrated with field experiment data.

4.2.5 Groundwater Module

In this module, we conduct the water balance calculation after having finished calculating percolation from the soil layer over the groundwater layer, the water-pumping output through wells, the outflow of springs, the capillary moisture into the above soil layer and the groundwater lateral seepages between different land-types. Ultimately, we get the variance process of the groundwater table over time and the excess surface water quantity.

In this module, the model includes groundwater drainage (DR) predominantly from irrigated to non-irrigated land due to irrigation, the groundwater exchange between irrigated and non-irrigated land (IIG), that between non-irrigated land types with different surfaces (GCH), and change in groundwater depth (ΔH).

Among them, $DR = PD \times A \times (H_0 - IH)$, PD is the drainage coefficient; A is the influence area of a drain ditch, km^2 ; H_0 is the depth of drain ditch, meters; IH is the groundwater depth in irrigated land, output value, meters. $IIG = CWL * (H - IH) * AI$, CWL is the groundwater exchange coefficient between irrigated land and non-irrigated land; H is the mean groundwater depth in irrigated land and non-irrigated land, output value, meters; AI is the area of irrigated land, km^2 . $GCH_i = PGW * (H_i - h_i - HNI) * A_i$, i stands for different land type, such as marsh, forest and grass land, bare land etc.; PGW is the groundwater exchange coefficient between different non-irrigated land use types; H_i is the altitude of the i th non-irrigated land use type, meters; h_i is the groundwater depth in the i th non-irrigated land type, output value, meters; HNI is the mean value of $(H_i - h_i)$ in all non-irrigated lands, because the exchange rate in the groundwater is very slow, here we use the mean value of $(H_i - h_i)$ in all non-irrigated lands instead of the mean one between two adjacent land use types, meters; A_i is the area of the i th non-irrigated land type, km^2 . $\Delta H = \frac{\Delta GW}{1,000\mu}$, ΔGW is the change in groundwater storage, $\Delta GW = GW_1 - GW_0$, where GW_0 is the groundwater storage at the beginning of the calculating interval while GW_1 is that at the end of the calculating interval; μ is the soil specific yield.

4.3 Model Parameters Calibration Method

We designed a new model calibration method for DHMHO according to the characteristics in water cycle simulation in the desert oasis, as shown in Eqs. 3 and 4.

First, determine the initial values of parameters by way of investigation or by experience or by using values from other similar research areas;

Second, sort the annual data sequence of the Xiaota Hydrometric Station in descendent order and calculate their annual empirical frequency.

Third, begin the iteration of parameters adjustment with Eqs. 3 and 4.

Detailed calibration process is shown as Fig. 12.

Where, i is the order number from year 1971 to year 1995; j is the order number of parameter; $xtaof(i)$ refers to the empirical frequency of the annual outflow observed in the Xiaota Hydrometric Station; eff is a coefficient used to adjust the parameter

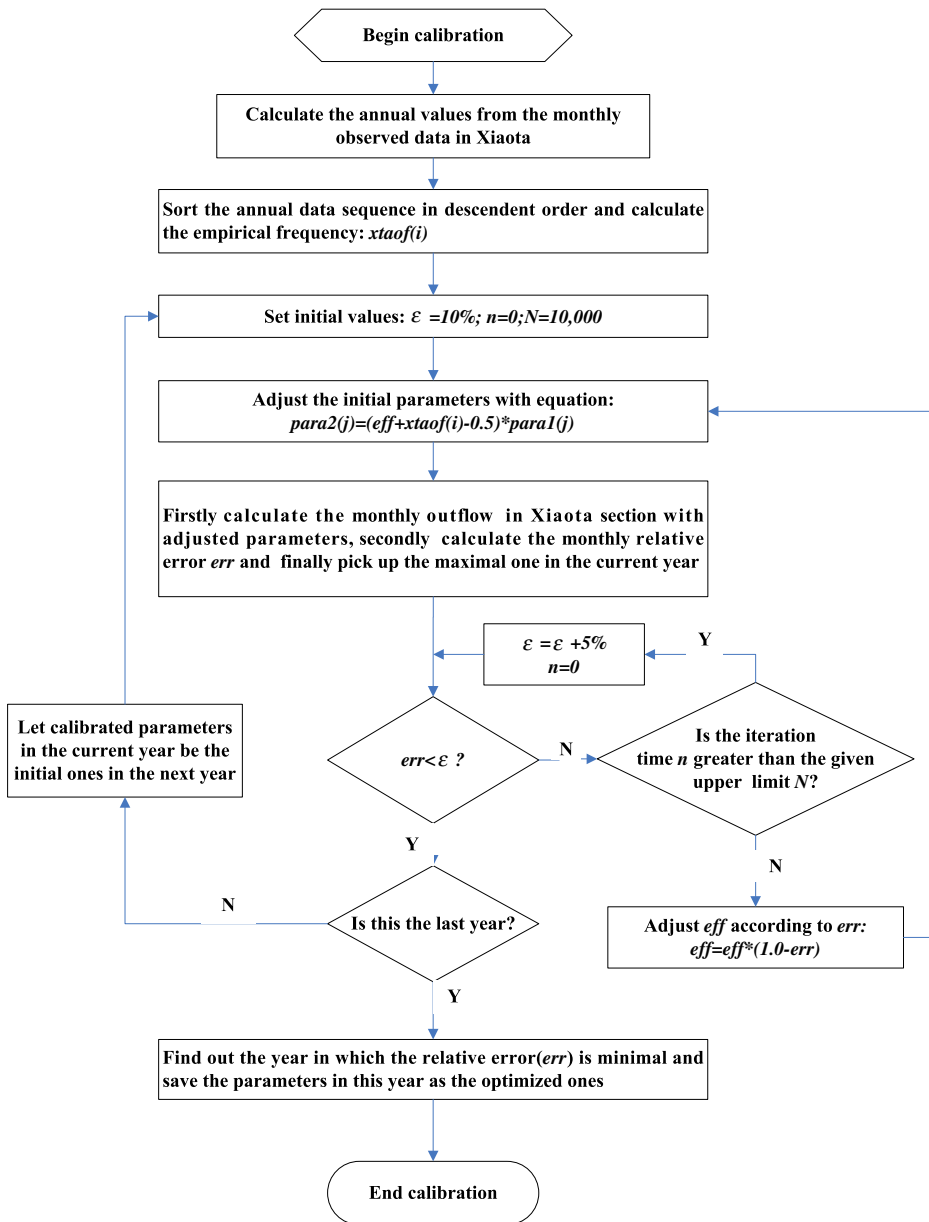


Fig. 12 Flow chart of parameters calibration in river module. Where, i is the order number from year 1971 to year 1995; j is the order number of parameter; $xtaof(i)$ refers to the empirical frequency of the annual outflow observed in the Xiaota Hydrometric Station; eff is a coefficient used to adjust the parameter which is determined by the relative error(err) between the observed monthly outflow and simulated one; $para2(j)$ is the adjusted parameter; $para1(j)$ is the initial one; ε is the upper limit of relative error(err); n is iteration time; N is the maximum iteration time

which is determined by the relative error(*err*) between the observed monthly outflow and simulated one; *para2*(*j*) is the adjusted parameter; *para1*(*j*) is the initial one; ε is the upper limit of relative error(*err*); *n* is iteration time; *N* is the maximum iteration time.

$$para2(j) = (eff + xtaof(i) - 0.5) \times para1(j) \tag{3}$$

$$eff = eff \times (1.0 - err) \tag{4}$$

Equation 3 is the empirical equation that we designed for DHMHO based on theories in hydrological statistics in the course of our study of the calibration methods. When *xtaof*(*i*) is greater than 50% i.e. the observed outflow value in Xiaota is less than the normal one, the parameter *para2*(*j*) is enlarged; otherwise, it is reduced.

5 Results

DHMHO has six main parameters including: moisture content in upper-layer soil (*WUM*), moisture content in lower-layer soil (*WMM*), the groundwater drainage coefficient (*PD*), the groundwater exchange coefficient between irrigated land and non-irrigated land (*CWL*), the groundwater exchange coefficient between non-irrigated lands (*PGL*) and the soil specific yield (μ).

To verify and to properly apply the model, model parameters were firstly calibrated with the parameter-calibration method in Fig. 12 on the basis of the observed monthly data from the Xiaota Hydrometric Station from year 1971 to year 1995. The calibration results are listed in Table 2. Then, sensitivity analysis of the model parameters was conducted to have a look at the stability of those parameters. Finally, the rationality of DHMHO was checked with the two observed data sequences: one is the varying process of groundwater depth; the other is the annual outflow sequence from the Xiaota Hydrometric Station, meanwhile, the model simulation errors were also analyzed.

5.1 Model Parameters Sensitivity Analysis

Introduce an uncertainty range of (−50% to 50%) for every calibrated model parameter, then the corresponding influence on the outflow in Xiaota were recorded, as shown in Table 3.

Table 2 Optimized DHMHO parameters for Hotan Oasis

Parameter	Calibration
Moisture storage capacity in upper-layer soil: WUM/mm	20
Moisture storage capacity in lower-layer soil: WMM/mm	300
Groundwater drainage coefficient: PD	0.16
Groundwater exchange coefficient between irrigated and non-irrigated land: CWL	0.25
Groundwater exchange coefficient between non-irrigated lands: PGW	0.50
Soil specific yield: μ	In loam In sandy loam
	0.05 0.08

Table 3 DHMHO parameters sensitivity

Parameter	-50%	-30%	-10%	-5%	0	+5%	+10%	+30%	+50%
WUM	0.14	0.09	0.03	0.02	0	-0.02	-0.04	-0.10	-0.14
WMM	0.88	0.42	0.12	0.06	0	-0.05	-0.10	-0.27	-0.40
PD	-1.03	-0.56	-0.12	-0.06	0	0.05	0.10	0.27	0.40
CWL	1.13	0.52	0.14	0.07	0	-0.06	-0.12	-0.34	-0.54
PGL	-0.31	-0.16	-0.04	-0.02	0	0.02	0.04	0.10	0.14
μ	0.84	0.18	0.06	0.03	0	-0.03	-0.06	-0.31	-0.42

As to the uncertainties, influences of all the six model parameters on the outflow simulations seem not marked. Change in *CWL* has the greatest influence on the simulations, maximum of which is making the outflow in Xiaota increase by 1.13%. Sensitivity analysis implies that the model parameters are stable, and uncertainties of these optimum parameters have little impact on the model simulations.

5.2 Model Rationality Check and Error Analysis

1. The varying process of groundwater depth

Because the observed data of groundwater depth from the year 2001 to 2003 is entire, we decide to compare the mean monthly values simulated by DHMHO during this period with those observed in the research areas, to analyze whether there exists irrationality in the simulation. Table 4 presents the mean monthly values of groundwater depth from year 2001 to year 2003 and gives analysis of the simulation errors.

Table 4 shows that all absolute relative errors in 12 months are within 25%; there are 11/12 of points with absolute relative errors less than 20%, 9/12 less than 10%. Among the 12 months the relative error in May is the greatest. The reason may be that May is at the height of the dry season and many scattered diversion-gaps, made privately by local farmers without any permission from the government, appear in the Hotan River, in addition, because of the poor management of the river, the detailed data about water quantity diverted through these diversion-gaps can not be collected, which affects the simulation precision of DHMHO. The water diverted from river is mainly used for irrigation and most seeps into underground ultimately, which makes the groundwater table in the irrigated land rise. Perhaps for the reason mentioned above, the simulated values from April to June are all less than the observed ones.

2. The Annual Outflow in the Xiaota Hydrometric Station

We have now the outflow data from the Xiaota Hydrometric Station available from year 1971 to year 2003, part of which (data from year 1971 to year 1995) has been used to calibrate the model parameters. Here we will use the remaining part (data from year 1996 to year 2003) to check the simulation rationality and analyze the simulation errors.

In this part, we first conduct the simulation with DHMHO and then compare the simulated outflow values with the observed ones to check whether there exists any irrationality, and finally analyze the simulation errors. In the course of the error-analysis, we evaluate the efficiency of DHMHO based on monthly data from year 1996 to year 2003 by means of the Nash–Sutcliffe efficiency coefficient (NSEC, Nash

Table 4 Mean monthly values of groundwater depth from 2001 to 2003 and corresponding errors

Month number	1	2	3	4	5	6	7	8	9	10	11	12	Average	Sum
Simulated value/m	2.35	2.48	2.49	2.47	2.45	2.37	2.30	2.26	2.31	2.38	2.44	2.51	2.40	
Observed value/m	2.89	2.73	2.56	2.95	3.17	2.63	2.15	2.10	2.13	2.30	2.43	2.38	2.54	
Err/%	-18.71	-9.33	-2.45	-16.14	-22.71	-9.94	6.66	7.68	8.43	3.65	0.36	5.64	-5.28	
Abs(err) <5%?	No	No	Yes	No	No	No	No	No	No	Yes	Yes	No		3
Abs(err) <10%?	No	Yes	Yes	No	No	Yes	Yes	Yes	Yes	Yes	Yes	Yes		9
Abs(err) <20%?	Yes	Yes	Yes	Yes	No	Yes	Yes	Yes	Yes	Yes	Yes	Yes		11
Abs(err) <25%?	Yes	Yes	Yes	Yes	Yes	Yes	Yes	Yes	Yes	Yes	Yes	Yes		12

In Table 4, *err* stands for relative error and *abs(err)* stands for absolute relative error; ave. stands for mean value; sum refers to total number of points that match the conditions left, or total number of 'yes'.

Table 5 Simulation errors analysis

Year	1996	1997	1998	1999	2000	2001	2002	2003	Average
Simulated value/ 10^8 m^3	8.30	3.89	5.50	9.50	7.81	13.25	8.43	10.56	8.41
Observed value / 10^8 m^3	8.60	5.57	7.92	8.44	8.18	12.20	7.81	10.25	8.62
Absolute error/ 10^8 m^3	0.30	1.68	2.43	-1.06	0.37	-1.05	-0.62	-0.31	0.21
Relative error /%	3.55	43.06	44.14	-11.18	4.69	-7.92	-7.32	-2.98	2.56
Absolute relative error/%	3.55	43.06	44.14	11.18	4.69	7.92	7.32	2.98	2.56
Annual NSEC	0.78	0.25	0.77	0.95	0.99	0.99	0.78	0.90	0.80

and Sutchliffe 1970) which can measure how well the simulated values agree with the observed ones (Table 5).

From the correlation of simulated and measured values (Fig. 13), we can see that the model has a high precision in large outflow (in the higher part of the line) simulation than that in small outflow (in the lower part of the line) simulation. But on the whole, the processes of the two series (Fig. 14) show the model can give satisfying performances in most simulations.

Table 5 shows that in the year 1997, there are a greater simulation error (43.06%) and a smaller annual NSEC (0.25). In the year 1998, there is a greater relative error (44.14%, ranking first in all years), but the annual NSEC in this year is great (0.77). In the rest years there are smaller relative errors and greater annual NSECs.

As for the relative error in Table 5, the minimal value appears in the year 2003 (-2.98%) and the maximal value in 1998. The relative error in 1997 ranks second in all years from 1996 to 2003. From Table 5, we can see that 37.5% of relative errors are less than 5%, 62.5% of that are less than 10% and 75.0% of that are less than 20%. The average relative error in eight years is 2.56%. All mentioned above suggest that DHMHO has a high precision and is able to be put into practice.

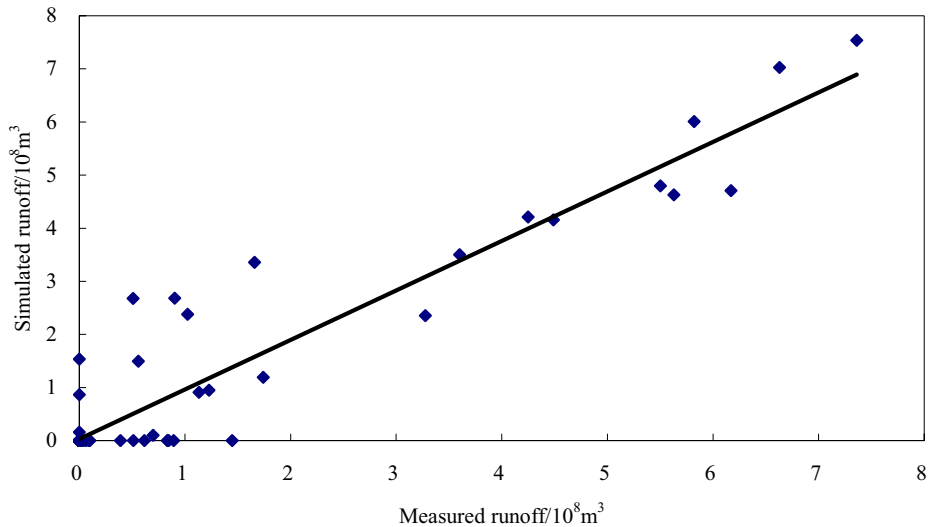


Fig. 13 Correlation of simulated runoff by DHMHO and measured runoff in Xiaota Hydrometric Station

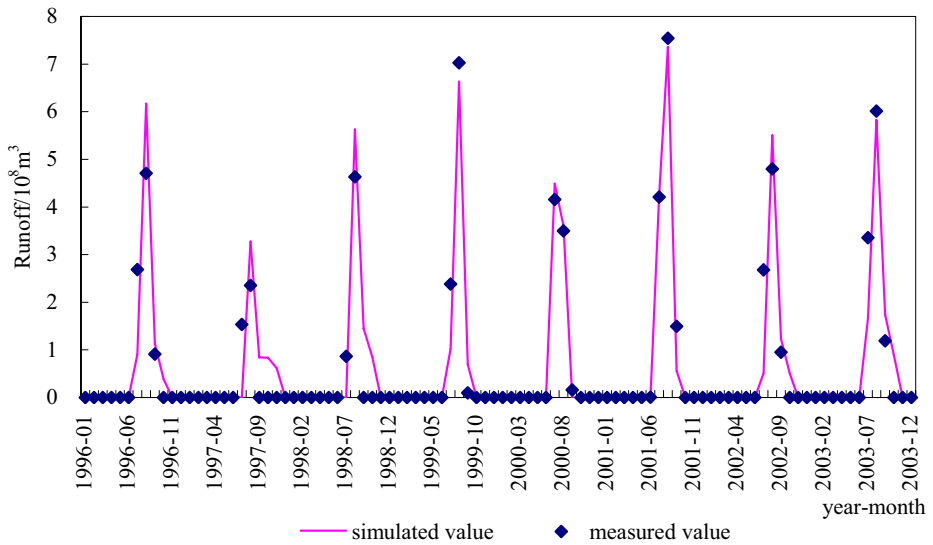


Fig. 14 Simulated runoff by DHMHO and measured runoff in Xiaota Hydrometric Station

In the year 2000 and 2001, DHMHO has the greatest NSEC (0.99). In all years except for 1997, the model has greater NSECs (>0.70) and on the whole, the model has an average NSEC of 0.80. The NSECs in Table 5 indicate the model is feasible for practical use.

From the analysis in this section, we can draw the conclusion that DHMHO has a high precision in the long-term simulation and can be used to simulate the water transformation in a desert oasis, helping local people to gain a better knowledge of local water resources and the status quo of water use and allocation.

5.3 Application of DHMHO to the Hotan Oasis

According to the “IPCC (Intergovernmental Panel on Climate Change) Fourth Assessment Report”, climate of the Oasis in the next decade (2011–2020) was predicted with the scenario “committed climate change”. It implies that mean annual rainfall amount in the next decade will increase compared with that in this decade (2001–2010) while mean annual relative humidity and air temperature will change little. Analysis on history data suggests irrigated land area in the Oasis has an increasing trend because of the regional population expansion. Yet the water quantity required by the irrigated vegetation has been reducing because of adoption of agricultural water-saving technics in recent years. All these will contribute to the climate and water cycle in the Hotan Oasis to some degrees.

Taking all those into account, we simulated the water transformation and dissipation of the next decade in the Hotan Oasis with DHMHO. The simulations suggest:

1. The mean evapotranspiration of the next decade in the Hotan Oasis will be $1.39 \times 10^9 \text{ m}^3$ accounting for 54.72% of total diverted water, among which: $0.29 \times 10^9 \text{ m}^3$ (20.86%) will be evaporated from the surface of water bodies

including river, reservoir/lake, marsh etc.; $0.87 \times 10^9 \text{ m}^3$ (62.59%) from irrigated vegetation encompassing crop and irrigated forest and grass; $0.027 \times 10^9 \text{ m}^3$ (1.94%) from non-irrigated forest and grass; $0.20 \times 10^9 \text{ m}^3$ (14.39%) from bare land.

This shows that in the years from 2011 to 2020 there will be $1.39 \times 10^9 \text{ m}^3$ of water in the Hotan Oasis moving into the atmosphere through varies of surface. According to Lundqvist and Falkenmark (2000), blue water is of direct use, liquid, visible water while green water is that of consumptive use, invisible, in the evapotranspiration process involved in plant production. In the next decade on average $0.90 \times 10^9 \text{ m}^3$ of blue water will be finally consumed by transformation into green water in the Hotan Oasis (evapotranspired by plant).

2. As to the whole Hotan River (including the reaches out of the Hotan Oasis), on average there will be $4.72 \times 10^9 \text{ m}^3$ of inflow among which 2.11×10^9 will be diverted into the Hotan Oasis and 0.052×10^9 into the areas out of the Hotan Oasis, $1.06 \times 10^9 \text{ m}^3$ of river water will be evaporated directly from river water surface, $1.04 \times 10^9 \text{ m}^3$ of river water seeps into underground. There also will be $1.11 \times 10^9 \text{ m}^3$ of outflow with $0.49 \times 10^9 \text{ m}^3$ of water quantity including recession water (i.e. part of diverted river water returning directly to river) and drainage water from irrigated crop land.

The above-mentioned indicates that 22.46% of the inflow of the Hotan River will be evaporated and 22.03% will seep into underground, i.e., only 55.51% of inflows of the river are left for the use of the Hotan Oasis and for recharging the downstream Tarim River.

3. On average, in the next decade, the whole Hotan Oasis will divert $2.54 \times 10^9 \text{ m}^3$ of water among which 2.11×10^9 will be from river (83.07%), 0.23×10^9 from springs (9.06%), 0.17×10^9 from reservoirs (6.69%), 0.026×10^9 from wells (1.02%)—in the next decade, the Hotan River will still be the dominant water-supply source and therefore, protection of the Hotan River will be of significant importance.

Of the total diverted water, 0.22×10^9 will flow into reservoirs (8.66%), 0.27×10^9 will be evapotranspired from canal system (10.63%), 0.81×10^9 seep into underground from canal system (31.89%) and 0.19×10^9 flow back into river from canal system (7.48%)—that is to say, 50% of the diverted water will lose in the canal system, only 1.02×10^9 can arrive at irrigated land for the agricultural use (40.16%). That suggests the canal system in the Hotan Oasis will still be the greatest water-loss site; therefore, to strengthen the management on the canal system, i.e. to reduce the futile evapotranspiration, seepage and recession water from the canal system effectively, will be of great significance.

4. In the next decade, on average $1.02 \times 10^9 \text{ m}^3$ of surface water will be diverted into irrigated land. Plus $0.14 \times 10^9 \text{ m}^3$ of capillary water from groundwater will be utilized by plant. Among all, there will evapotranspire $0.87 \times 10^9 \text{ m}^3$ (75.0%), seep into underground $0.26 \times 10^9 \text{ m}^3$ (22.4%) and store in the vadose zone $0.023 \times 10^9 \text{ m}^3$ (2.0%). That means evapotranspiration in irrigated land will be dominant in all water-dissipative items.

5. In the next decade, of the water flowing into reservoirs ($0.22 \times 10^9 \text{ m}^3$), 0.022×10^9 will evaporate from reservoir water surface (10.0%), 0.020×10^9 seep into underground from reservoirs (9.1%), 0.0076×10^9 store in reservoirs (3.5%) and 0.167×10^9 flow out of reservoirs for the use of Hotan Oasis (75.9%). This shows that the reservoir water in the Hotan Oasis is mostly used to supply water for the oasis, but evaporation and seepage of reservoirs can not be ignored (accounting for 19.1% of the reservoir inflows).

In the next decade, of the groundwater in the Hotan Oasis, recharging water will be $1.28 \times 10^9 \text{ m}^3$: Lateral seepage into the oasis will be 0.13×10^9 (10.2% of the recharging water), river seepage into the oasis will be 0.055×10^9 (4.3%), canal system seepage in the oasis will be 0.81×10^9 (63.3%), irrigated land seepage will be 0.26×10^9 (20.3%), and reservoirs seepage there will be 0.020×10^9 (1.6%); discharging water will be $1.19 \times 10^9 \text{ m}^3$: lateral seepage out of the Hotan Oasis will be 0.22×10^9 (18.5% of the discharging water), upward capillary water in the Hotan Oasis will be 0.14×10^9 (11.8%), evapotranspiration from non-irrigated forest and grass will be 0.027×10^9 (2.3%), evaporation from bare land will be 0.20×10^9 (16.8%), well-pumped groundwater will be 0.026×10^9 (2.2%) and spring water will be $0.58 \times 10^9 \text{ m}^3$ (48.7%). Drainage from irrigated land will be $0.21 \times 10^9 \text{ m}^3$ and the water exchanges between irrigated land and non-irrigated land will be $0.60 \times 10^9 \text{ m}^3$.

It means that on average $0.61 \times 10^9 \text{ m}^3$ of groundwater will be transformed into surface water annually, $0.36 \times 10^9 \text{ m}^3$ of groundwater into vapor moving into the atmosphere of the Hotan Oasis and $1.15 \times 10^9 \text{ m}^3$ of surface water and soil moisture (from the vadose zone of irrigated land) will be transformed into groundwater annually in the 10 years.

Horizontally, lateral seepage into the oasis ($0.13 \times 10^9 \text{ m}^3$) will be less than that out of the oasis ($0.22 \times 10^9 \text{ m}^3$); vertically, seepage from surface water into groundwater ($1.15 \times 10^9 \text{ m}^3$) will be greater than the water quantity from groundwater to surface water ($0.61 \times 10^9 \text{ m}^3$). That means the use of surface water should moderately be reduced and exploitation of groundwater should be enhanced because the soil salinization status quo in the Hotan Oasis is severe and there will be great potential of groundwater exploitation—if not or little just as nowadays, evapotranspiration will be very great and the accumulation of salinity with intense evapotranspiration will be severer and severe. Therefore, exploitation degree of groundwater should be strengthened—empirically, about annual $0.2\sim 0.3 \times 10^9 \text{ m}^3$ of groundwater exploitation will be adequate in the next decade.

6. The mean annual groundwater depth in the Hotan Oasis in the next decade will be 5.31 m. That in irrigated land will be 5.21 m and that in non-irrigated land be 5.45 m.

In summary, to ensure the sustainable development of the Hotan Oasis, various water-saving technologies have to widely be taken into account:

Firstly, it should be the most important to reduce water loss in canal system by improving canal water-use efficiency through various of canal lining project and water-surface area reducing project.

Secondly, reducing the diverted surface water quantity and meanwhile increasing the utilizing quantity of groundwater, and hence to lower the groundwater table to reduce the futile evaporation in the Hotan Oasis.

Thirdly, moving the reservoirs in the plain oasis to the mountain areas will notably reduce water surface area in the Hotan Oasis and therefore reduce the reservoir evaporation and seepage effectively.

Last but not the least, various water-saving technologies in the cropland must be further taken into account. In addition, the adjustment of cropping structure and the selection of soil quality improvement methods also should be considered.

All the results analyzed above are expected to contribute to the sustainable development of the Hotan Oasis and the gradual improvement of residents' living standard there.

6 Conclusions

We presented the Dissipative Hydrological Model for the Hotan Oasis (DHMHO) based on the arid plain oasis model developed by the research cooperation group which consisted of Tsinghua University, Xi'an University of Technology, Xinjiang Agricultural University, and on the analyzing the data accumulated in the long-term study on the characteristics of moisture transformation and movement, climate, geology and vegetation etc. in arid desert areas and on that of water–land resources in the Hotan Oasis.

A new parameter-calibrating method was designed specially for DHMHO, with which, We calibrated the parameters of DHMHO utilizing the observed outflow data (from year 1971 to year 1995) at the Xiaota Hydrometric Station—the sole control hydrometric station in the Hotan River and in the end, saved the optimized parameters for future model-simulation use.

With DHMHO containing the optimized parameters, we respectively simulated the groundwater depth from year 2001 to 2003 and outflow in Xiaota from year 1996 to 2003 against which we checked the rationality of our model and analyzed the simulation errors.

Finally, we applied this model to the Hotan Oasis to simulate water transformation and dissipation in future from year 2011 to 2020 according to which, we analyzed the mean annual values in the 10 years.

The results show that DHMHO has a high simulation precision and is a helpful tool for people in the oasis to establish reasonable policies concerning the exploitation and allocation of water–land resources in order to gradually improve the quality of the local ecology and environment and make the local social economy develop sustainably. However, DHMHO is only applicable to those arid desert oases similar to the Hotan Oasis, and there may exist some uncertainties in parameter estimation and simulation process. In the future, emphasis should be laid in collection of much more detailed relevant data in the arid desert to further explore the inner water cycle rules there, and in establishment of new methods for parameter estimation and simulating process optimization to reduce uncertainties and elevate the model precision.

Acknowledgements This study was supported by Project of the Natural Science Foundation of China (No.50779052). Many thanks to Prof. Dong Xin-guang and Prof. Hudan-Tumarbai from Xinjiang Agriculture University who participated the research cooperation group as scholars and contributed a lot to the research; to all the colleagues from Tsinghua University, Xi'an University of Technology and Xinjiang Agricultural University who undertook research tasks and devoted time and wisdom to this study.

References

- Borah DK, Bera M (2003) Watershed-scale hydrologic and nonpoint-source pollution models: review of mathematical bases. *Trans ASAE* 46(6):1553–1566
- Casey MJ (1999) The effect of watershed subdivision on simulated hydrologic response using the nrcc tr-20 model. Master thesis, University of Maryland
- Chai XL, Guo SL, Peng DZ, Zhang HG (2006) A study on the application of IHACRES model in runoff simulation in ungauged basins. *J China Hydrol* 26(2):30–33
- Chen JF, Lee CH, Yeh TC, Yu JL (2005) A water budget model for the Yun-Lin plain, Taiwan. *Water Resour Manag* 19:483–504
- Dye PJ, Croke BFW (2003) Evaluation of streamflow predictions by the IHACRES rainfall–runoff model in two South African catchments. *Environ Model Softw* 18:705–712
- Harbaugh AW, Banta ER, Hill MC, McDonald MG (2000) MODFLOW-2000, the U.S. geological survey modular ground-water model—user guide to modularization concepts and the ground-water flow process. U.S. Geological Survey, Open-File Report 00-92, Reston, Virginia
- Hernandez M, Miller SN, Goodrich DC et al (2000) Modeling runoff response to land cover and rainfall spatial variability in semi-arid watersheds. *Environ Monit Assess* 64:285–298
- Hu HP, Tang QH, Lei ZD, Yang SX (2004) Runoff–evaporation hydrological model for arid plain oasis, 1, the model structure. *Adv Water Sci* 15(2):140–145
- Jakeman AJ, Littlewood IG, Whitehead PG (1990) Computation of the instantaneous unit hydrograph and identifiable component flows with application to two small upland catchments. *J Hydrol* 117:275–300
- Lei ZD, Yang SX, Xie SC (1988) Soil water kinetics. Tsinghua University Press, Beijing
- Li QF, Gowing J (2005) A daily water balance modelling approach for simulating performance of tank-based irrigation systems. *Water Resour Manag* 19:211–231
- Loukas A, Mylopoulos N, Vasiliades L (2007) A modeling system for the evaluation of water resources management strategies in Thessaly, Greece. *Water Resour Manag* 21:1673–1702
- Lundqvist J, Falkenmark M (2000) Editorial: towards hydrosolidarity: focus on the upstream–downstream conflicts of interests. *Water Int* 25(2):168–171
- Meng CH, Xia J (2004) Research on the water storage of soil reservoir. *Water Saving Irrigation* 4:8–10
- Nash JE, Sutcliffe JV (1970) River flow forecasting through conceptual models part I—a discussion of principles. *J Hydrol* 10:282–290
- Otles Z, Gutowski WJ (2005) Atmospheric stability effects on Penman–Monteith evapotranspiration estimates. *Pure Appl Geophys* 162:2239–2254
- Refsgaard JC, Sørensen HR, Mucha I et al (1998) An integrated model for the Danubian Lowland—methodology and applications. *Water Resour Manag* 12:433–465
- Shen B, Huang LM, Ruan BQ, Luo GM (2003) Study on the water cycling characteristics of the Hotan Oasis during the second half of last century. *J Hydraul Eng* 5:78–83
- Tang QH (2003) A study of dissipative hydrological model for arid plain oasis. Master thesis, Tsinghua University, Beijing
- Tang QH, Tian FQ, Hu HP (2004) Runoff–evaporation hydrological model for arid plain oasis, 2. Applications of the model. *Adv Water Sci* 15(2):146–150
- US Army Corps of Engineers (1997) Storage, treatment, overflow, runoff model. STORM user's manual. Hydraulic Engineering Center, David C A:170
- Wang AZ, Jin CJ, Liu JM, Pei TF (2006) A modified Hortonian overland flow model based on laboratory experiments. *Water Resour Manag* 20:181–192
- Wang RH, Zhang HZ, Ma YJ (2003) The reason for ecological fragility in the Hotan River basin. *Journal of Northwest University (Natural Science Edition)* 33(1):106–110
- Wanielista M, Kersten R, Eaglin R (1997) Hydrology—water quantity and quality control. Wiley, New York
- Xia J (2002) Nonlinear systematic theories and methods in hydrology. Wuhan University Press, Wuhan
- Xia J, Wang GS, Tan G, Ye AZ, Huang GH (2005) Development of distributed time-variant gain model for nonlinear hydrological systems. *Sci China D Earth Sci* 48(6):713–723
- Zhao RJ (1984) Basin hydrology modeling—Xin'anjiang model and Shanbei model. China Water-power Press, Beijing
- Zhao CS (2005) Study on dissipative hydrological model and its application to the Hotan oasis. Master thesis, Xi'an University of Technology, Xi'an